while no Gs protein could be detected in the culture medium (Figs. 4 and 8). On the other hand, in the full-length G cDNA-transfected cultures, the ratio of G_B-form on the cell surface was a little higher than that on the CT1-producing cells, but only a very small amount of Gs protein was detected in the culture fluid (Figs. 4 and 8). These facts do not necessarily disprove the idea that Gs proteins are produced from the G_C form of G protein exposed on the cell surface. In the case of CT1 protein expression, the amount of cell surface-exposed G_C-form of CT1 protein would not be sufficient for detecting the Gs protein shedding, or most of the CT1 proteins could have been in the G_D form.

In this study, we also investigated another C-terminal-deficient mutant (GΔTC; deficient in 76 amino acids from the C-terminus), which was originally prepared to establish a model system for studying the Gs protein production. In contrast to the Gs protein, however, the GΔTC could not be detected in the extracellular space, nor exported from the rER and retained in the cell. This observation was further confirmed by using anti-BiP antibody; GΔTC was shown to be associated with BiP, which is known to work as a molecular chaperone for correct folding of many kinds of glycoproteins in the rER (Fig. 5). Wojczyk et al. (28, 29) reported that a C-terminal-truncated form of the rabies virus G protein (T434), which comprised 433 amino acids, was released from the transfected cells and was immunogenic to animals. They also suggested that the glycosylation might be affected differently depending on the C-terminal structure of each mutant, and the optimal sites should be glycosylated in order to be normally processed and transported to the cell surface or to be shed from the cell (25, 29). Gaudin et al. (4) also reported similar results with another C-terminal-deficient mutant ($G_{1\text{-}439}$), which was secreted as a monomer that displayed the antigenic characteristics of the I-form (inactive form). One possibility for the observed difference in the intracelluar behavior between GΔTC and T434 or $G_{1\text{-}439}$ mutants might have come from their different C-terminal structures; T434 and $G_{1\text{-}439}$ mutants had four and nine more amino acids at the C-terminus than GΔTC, respectively. These differences imply that several amino acids in the ectodomain locating proximal to the transmembrane domain of the G protein might play an important role in correct folding and antigenic maturation of the protein.

We are grateful to Dr. Tadafumi S. Tochikura for his advice and discussions in manuscript preparation and to Miss Ai Matsumura for her assistance in manuscript preparation. This study was supported by a donation from the Kyoto Biken Laboratories, Inc. (Uji, Kyoto, Japan).

References

1) Chen, C., and Okayama, H. 1987. High-efficiency transformation of mammalian cells by plasmid DNA. Mol. Cell. Biol. **7**: 2745–2752.
2) Dietzschold, B., Wiktor, T., Wunner, W.H., and Varrichio, A. 1983. Chemical and immunological analysis of the rabies soluble glycoprotein. Virology **124**: 330–337.
3) Gaudin, Y. 1997. Folding of rabies virus glycoprotein: epitope acquisition and interaction with endoplasmic reticulum chaperones. J. Virol. **71**: 3742–3750.
4) Gaudin, Y., Moreira, S., Benejean, J., Blondel, D., Flamand, A., and Tuffereau, C. 1999. Soluble ectodomain of rabies virus glycoprotein expressed in eukaryotic cells folds in a monomeric conformation that is antigenically distinct from the native state of the complete, membrane-anchored glycoprotein. J. Gen. Virol. **80**: 1647–1656.
5) Gaudin, Y., Ruigrok, R.W., and Brunner, J. 1995. Low pH-induced conformational changes in viral fusion proteins: implications for fusion mechanism. J. Gen. Virol. **76**: 1541–1556.
6) Gaudin, Y., Ruigrok, R.W., Tuffereau, C., Knossow, M., and Flamand, A. 1992. Rabies virus glycoprotein is a trimer. Virology **187**: 627–632.
7) Gaudin, Y., Ruigrok, R.W., Knossow, M., and Flamand, A. 1993. Low-pH conformational changes of rabies virus glycoprotein and their role in membrane fusion. J. Virol. **67**: 1365–1372.
8) Gaudin, Y., Tuffereau, C., Durrer, P., Flamand, A., and Ruigrok, R.W.H. 1995. Biological function of the low-pH, fusion-inactive conformation of rabies virus glycoprotein (G): G is transported in a fusion-inactive state-like conformation. J. Virol. **69**: 5528–5534.
9) Irie, T., Matsùda, Y., Honda, Y., Morimoto, K., and Kawai, A. 2002. Studies on the escape mutants of rabies virus which are resistant to the neutralization by a highly conserved conformational epitope-specific monoclonal antibody #1-46-12. Microbiol. Immunol. **46**: 449–461.
10) Kankanamge, P.J., Irie, T., Mannen, K., Tochikura, T.S., and Kawai, A. 2003. Mapping of the low pH-sensitive conformational epitope of rabies virus glycoprotein recognized by a monoclonal antibody #1-30-44. Microbiol. Immunol. **47**: 507–519.
11) Kankanamge, P.J., Irie, T., Shoji, J., Tochikura, T.S., and Kawai, A. 2003. Further characterization of the rabies virus glycoproteins produced by virus-infected and G cDNA-transfected cells using a monoclonal antibody, #1-30-44, which recognizes an acid-sensitive epitope. Microbiol. Immunol. **47**: 337–349.
12) Kawai, A. 1977. Transcriptase activity associated with rabies virion. J. Virol. **24**: 826–835.
13) Kawai, A., and Matsumoto, S. 1981. Production of spikeless particles of the rabies virus under conditions of low pH. Virology **108**: 267–276.
14) Kawai, A., and Takeuchi, K. 1992. Temperature-sensitivity of the replication of rabies virus (HEP-Flury strain) in BHK-21 cells. I. Alteration of viral RNA synthesis at the elevated temperature. Virology **186**: 524–532.

15) Kawai, A., Toriumi, H., Tochikura, T.S., Honda, Y., and Morimoto, K. 1999. Nucleocapsid formation and/or subsequent conformational change of the rabies virus nucleoprotein (N) is a prerequisite step for acquisition of its phosphatase-sensitive epitope recognized by monoclonal antibody 5-2-26. Virology **263**: 395–407.
16) Laemmli, U.K. 1970. Cleavage of structural proteins during the assembly of the head of bacteriophage T4. Nature **227**: 680–685.
17) Lentz, T.L., Wilson, P.T., Hawrot, E., and Speicher, D.W. 1984. Amino acid sequence similarity between rabies virus glycoprotein and snake venom curare mimetic neurotoxins. Science **226**: 847–848.
18) Morimoto, K., Iwatani, Y., and Kawai, A. 1993. Shedding of Gs protein (a soluble form of the viral glycoprotein) by the rabies virus-infected BHK-21 cells. Virology **195**: 541–549.
19) Morimoto, K., Ni, Y.-J., and Kawai, A. 1992. Syncytium formation is induced in the murine neuroblastoma cell cultures which produce pathogenic type G protein of the rabies virus. Virology **189**: 203–216.
20) Morimoto, K., Ohkubo, A., and Kawai, A. 1989. Structure and transcription of the glycoprotein gene of attenuated HEP-Flury strain of rabies virus. Virology **173**: 465–477.
21) Nakahara, K., Ohnuma, H., Sugita, S., Yasuoka, K., Nakahara, T., Tochikura, T.S., and Kawai, A. 1999. Intracellular behavior of rabies virus matrix protein (M) is determined by the viral glycoprotein (G). Microbiól. Immunol. **43**: 259–270.
22) Ni, Y., Tominaga, Y., Honda, Y., Morimoto, K., Sakamoto, S., and Kawai, A. 1995. Mapping and characterization of a sequential epitope on the rabies virus glycoprotein which is recognized by a neutralizing monoclonal antibody, RG719. Microbiol. Immunol. **39**: 693–702.
23) Sakai, M., Kankanamge, P.J., Shoji, J., Kawata, S., Tochikura, T.S., and Kawai, A. 2004. Studies on the conditions required for structural and functional maturation of rabies virus glycoprotein (G) in G cDNA-transfected cells. Microbiol. Immunol. **48**: 853–864.
24) Seif, I., Coulon, P., Rollin, P.E., and Flamand, A. 1985. Rabies virulence: effect on pathogenicity and sequence characterization of rabies virus mutations affecting antigenic site III of the glycoprotein. J. Virol. **53**: 926–934.
25) Shakin-Eshleman, S.H., Wunner, W.H., and Spitalnik, S.L. 1993. Efficiency of N-linked core glycosylation at asparagine-319 of rabies virus glycoprotein is altered by deletions C-terminal to the glycosylation sequon. Biochemistry **32**: 9465–9472.
26) Tuffereau, C., Leblois, H., Benejean, J., Coulon, P., Lafay, F., and Flamand, A. 1989. Arginine or lysine in position 333 of ERA and CVS glycoprotein is necessary for rabies virulence in adult mice. Virology **172**: 206–212.
27) Whitt, M.A., Buonocore, L., Prehaud, C., and Rose, J.K. 1991. Membrane fusion activity, oligomerization, and assembly of the rabies virus glycoprotein. Virology **185**: 681–688.
28) Wojczyk, B., Shakin-Eshleman, S.H., Doms, R.W., Xiang, Z.Q., Ertl, H.C., Wunner, W.H., and Spitalnik, S.L. 1995. Stable secretion of a soluble, oligomeric form of rabies virus glycoprotein: influence of N-glycan processing on secretion. Biochemistry **34**: 2599–2609.
29) Wojczyk, B., Stwora-Wojczyk, M., Shakin-Eshleman, S.H., Wunner, W.H., and Spitalnik, S.L. 1998. The role of site-specific N-glycosylation in secretion of soluble forms of rabies virus glycoprotein. Glycobiology **8**: 121–130.

Microbiol. Immunol., 49(8), 757–770, 2005

Structural Difference Recognized by a Monoclonal Antibody #404-11 between the Rabies Virus Nucleocapsid (NC) Produced in Virus Infected Cells and the NC-Like Structures Produced in the Nucleoprotein (N) cDNA-Transfected Cells

Harufusa Toriumi, and Akihiko Kawai*

Department of Molecular Microbiology, Graduate School of Pharmaceutical Sciences, Kyoto University, Kyoto, Kyoto 606–8501, Japan

Received February 2, 2005; in revised form, May 19, 2005. Accepted May 23, 2005

Abstract: **We investigated structural changes in the rabies virus (HEP-Flury strain) nucleocapsid (NC) during the virus replication, for which we used two anti-nucleoprotein (N) monoclonal antibodies (mAbs), #404-11 (specific for a conformation-dependently exposed linear epitope) and #1-7-11 (specific for a conformational epitope which is exposed after the nucleocapsid formation). Both mAbs recognized the N protein of the viral NC, but not of the RNA-free N-P complex. The 1-7-11 and 404-11 epitopes could be mapped to the N-terminal and the C-terminal regions of N protein, respectively. Immunoprecipitation studies demonstrated that treatment of the NC either with the alkaline phosphatase or sodium deoxycholate (DOC) resulted in dissociation of most P proteins from the NC and in the reduced reactivity to mAb #404-11, but not to mAb #1-7-11. NC-like structures produced in the N cDNA-transfected cells displayed strong reactivity to mAb #1-7-11; however, reactivity to mAb #404-11 was very weak. And, coexpression with viral phosphoprotein (P) resulted in little increase in reactivity to mAb #404-11 of the NC-like structures, while the reactivity was significantly increased by cotransfection with P and the viral minigenome whose 3′- and 5′-end structures were derived from the viral genome. From these results, we assume that, although the 404-11 epitope is a linear one, the epitope-containing region is exposed only when N proteins encapsidate properly the viral RNA in collaboration with the P protein. Further, exposure of the 404-11 epitope region might be function-related, and be regulated by association and dissociation of the P protein.**

Key words: **Rabies virus nucleocapsid, Monoclonal antibody, Conformational change, Phosphorylation, Encapsidation, Structural maturation**

The negative-stranded RNA genome of the rabies virus encodes at least five species of structural proteins, nucleoprotein (N), nominal phosphoprotein (P), matrix protein (M), glycoprotein (G) and a large catalytic protein (L) in this order from its 3′-end to 5′-end. M and G proteins comprise the protein moiety of the viral envelope, while P and L proteins collaborate in viral RNA synthesis as non-catalytic and catalytic components of the viral RNA polymerase, respectively. The N protein is a virus-coded RNA-binding protein. After being complexed with the P protein, the N proteins in such RNA-free N-P complexes are involved in specific encapsidation of viral genomic RNA (25), forming a nucleocapsid (NC) in the virus infected cells, and are

Address correspondence to Dr. Akihiko Kawai, Department of Molecular Microbiology, Graduate School of Pharmaceutical Sciences, Kyoto University, Sakyo-ku, Kyoto, Kyoto 606–8501, Japan. Fax: +81–75–761–2698. E-mail: akawai@pharm.kyoto-u.ac.jp

Abbreviations: CBB, Coomassie brilliant blue; cDNA, complementary deoxyribonucleic acid; CIAP, calf intestine alkaline phosphatase; DOC, deoxycholate; G, glycoprotein; L, large subunit of viral RNA polymerase; M, matrix protein; mAb, monoclonal antibody; MEM, minimum essential medium; N, nucleoprotein; NC, nucleocapsid; NP-40, Nonidet-P 40; P, phosphoprotein; pAb, polyclonal antibody; PAGE, polyacrylamide gel electrophoresis; PBS, phosphate-buffered saline; RIPA, radioimmunoprecipitation assay; RNP, ribonucleoprotein; RVV-T7, T7 RNA polymerase gene-containing recombinant vaccinia virus; SDS, sodium dodecyl sulfate; Ser, serine residue.

then phosphorylated on the serine residue at position 389 (Ser-389) (14, 26) .

The encapsidation process is believed to be performed by N proteins in a consecutive manner of wrapping each group of several (probably six) nucleotides from one end to the other of the genome-sized RNA (11, 24). During the viral encapsidation process, the N proteins concomitantly undergo conformational changes, which could be recognized by anti-N mAb #5-2-26, #1-7-11 (14) and #404-11 (Kawai and Toriumi, unpublished observation), and they also receive a phosphate group at Ser-389. The mAb #404-11 recognizes a linear epitope of N protein (13); however, the N protein might have to take a specific conformation for being recognized by this mAb, because the RNA-free N-P complex is not recognized by the mAb (our unpublished observation). To differentiate the phosphorylated form of N protein from the unphosphorylated one, we reported that mAb #5-2-26 recognized only the phosphorylated form of the N protein that composes the viral NC (1, 13). The P protein may either leave the newly formed NC probably due to conformational changes of N protein, or it may reassociate with the NC by exchanging its binding site from the N-terminal side to the C-terminal domain (3, 5, 17, 21, 23). In the latter case, P proteins may also change their conformation, which could be recognized by an anti-P mAb #402-13 (21).

The encapsidation-related conformational change of the N protein might be a prerequisite event for being phosphorylated at Ser-389. However, such changes have not yet been investigated precisely, although there are some reports describing, for instance, identification of the N protein phosphorylation site (Ser-389; 1, 4, 26) and finding of a critical step of the phosphorylation (14).

In this study, we further performed some experiments to know more about the encapsidation process, including the encapsidation-related structural changes and phosphorylation at Ser-389 by using some anti-N mAbs (e.g., #5-2-26, #1-7-11 and #404-11). In this study, we noticed that mAb #404-11 differentiates the structural difference between the NC-comprising N proteins produced in the virus infected and the N cDNA-transfected cells. In other words, although the N proteins produced in the N cDNA-transfected animal cells were recognized by most of our conformational epitope-specific anti-N mAbs, most of them were not recognized by mAb #404-11, and then only very weakly. This point was also discussed from the viewpoint of the structural and conformational maturation of N protein during the viral replication process.

Materials and Methods

Viruses and cell culture. We used the BHK-adapted HEP-Flury and the Nishigahara RC-HL strains of rabies virus (6, 10, 18). Rabies virus propagation and plaque assay were performed using BHK-21 cells as described previously (12). The recombinant vaccinia virus (RVV-T7; received from Dr. Kohara, Tokyo Metropolitan Institute of Medical Science, Tokyo), containing the T7 phage RNA polymerase gene, was used to provide the T7 RNA polymerase for promoting the expression in animal cells of the rabies virus N and P cDNAs and their mutants inserted under the T7 promoter of expression vectors (pCDM8 and pET3a). BHK-21 cells were grown in Eagle's MEM supplemented with 5% calf serum and 10% Tryptose phosphate broth (Difco). Virus infected cultures were incubated in a maintenance medium composed of MEM and 3% fetal bovine serum.

Expression of N and P cDNAs and the minigenome. The N and P gene expression in animal cells was performed by inserting the cDNA downstream of the T7 promoter of pCDM8 (1, 20). The N cDNA clone of the Nishigahara RC-HL strain as well as the recombinant N cDNAs HEP/RC-HL (*Sty*I) and RC-HL/HEP (*Sty*I) were received from Dr. N. Minamoto (Gifu University, Gifu, Japan). Recombinant N cDNAs HEP/RC-HL (*Eco*T22I) and RC-HL/HEP (*Eco*T22I) were prepared by exchanging the counterparts of the N cDNA fragments of the HEP-Flury and Nishigahara RC-HL strains cut at *Eco*T22I site, and transferred to pET3a vector for expression under the control of T7 promoter. Vector constructs for expressing the recombinant N cDNAs HEP/RC-HL (*Sty*I) and RC-HL/HEP (*Sty*I) were the same as described previously (7, 8). The cDNAs encoding a phosphorylation-deficient point mutant N (S389A) and other deletion mutant N cDNAs were the same ones described previously (1). Minigenome expression was performed as follows: the rabies virus minigenome cDNA composed of the leader sequence, M and G genes and trailer region of the HEP-Flury strain, followed by the ribozyme sequence of hepatitis delta virus, was inserted into pGEM-3Z vector (Promega Corp.). The transcription from the vector was controlled by the T7 promoter.

Expression of the wild type cDNAs and their mutants as well as the minigenome was performed by transfecting the reconstructed expression vectors (molar ratio of the N cDNA, P cDNA and minigenome DNA was 1:1:1; when the minigenome was omitted; the empty vector DNA was included instead) to BHK-21 cell monolayers by a calcium phosphate method (2)

Table 1. Properties of anti-N mAbs used in this study

Condition of the N protein	Anti-N mAbs					
	#404-11 (L)[a]		#5-2-26 (L)		#1-7-11 (C)[b]	
	IP[c]	IB[d]	IP	IB	IP	IB
RNA-free N-P complex	−[e]	+	−	−	−	−
Nucleocapsid: intact	+	+	+	+	+	−
phosphatase-treated	−[e]	+	−	−	+	ND[f]

Properties of each mAb were summarized based on the studies described in our previous publicaions (1, 13, 14, 23).

[a] "L" denotes a linear epitope.

[b] "C" denotes a conformational epitope.

[c] Detection by immunoprecipitation.

[d] Detection by immunoblotting.

[e] Data was obtained in this study.

[f] Not done.

with RVV-T7 (see above) as described previously (1).

Antibodies. Anti-N monoclonal antibodies (mAbs) #5-2-26, #1-7-11 and #404-11 were the same ones described in our previous reports (1, 13, 14). Their properties are summarized in Table 1. The rabbit polyclonal antibodies (pAbs) against the rabies virus N and P proteins were also the same ones described previously (13, 20).

Radiolabeling of infected and cDNA-transfected animal cells. Rabies virus-infected and cDNA-transfected cells were preincubated for 30 min in a methionine-free medium, followed by incubation with L-[^{35}S]methionine (10 μCi/ml) for 4 to 6 hr. After being washed three times with PBS(−), cells were lysed in DOC-free RIPA(I) buffer.

Sucrose density gradient centrifugation. Infected cell lysates (0.5 ml) were applied onto a 10–40% sucrose density gradient (4.5 ml) and span at 25,000 rpm (85,000×*g*) for 120 min at 4 C. Then, the gradient was fractionated into 10 fractions and a bottom fraction (fraction #11) which was recovered by suspending the pellet in 0.5 ml RIPA (I) buffer. Fraction #1 was termed as the top fraction which contained the RNA-free N-P complex as reported previously (14). Fractions #6 and #7 contained the nucleocapsids (NC) (see Fig. 1; they were mixed for use as the NC fraction). In other experiments (e.g. immunoprecipitation studies; see below), the NC fraction was obtained mostly as a pellet through a 20% sucrose cushion as described before (14, 21).

Phosphatase-treatment of the nucleocapsid. Radiolabeled rabies virus-infected BHK-21 cells were lysed in a DOC-free RIPA(I) buffer (1% NP-40, 140 mM NaCl,

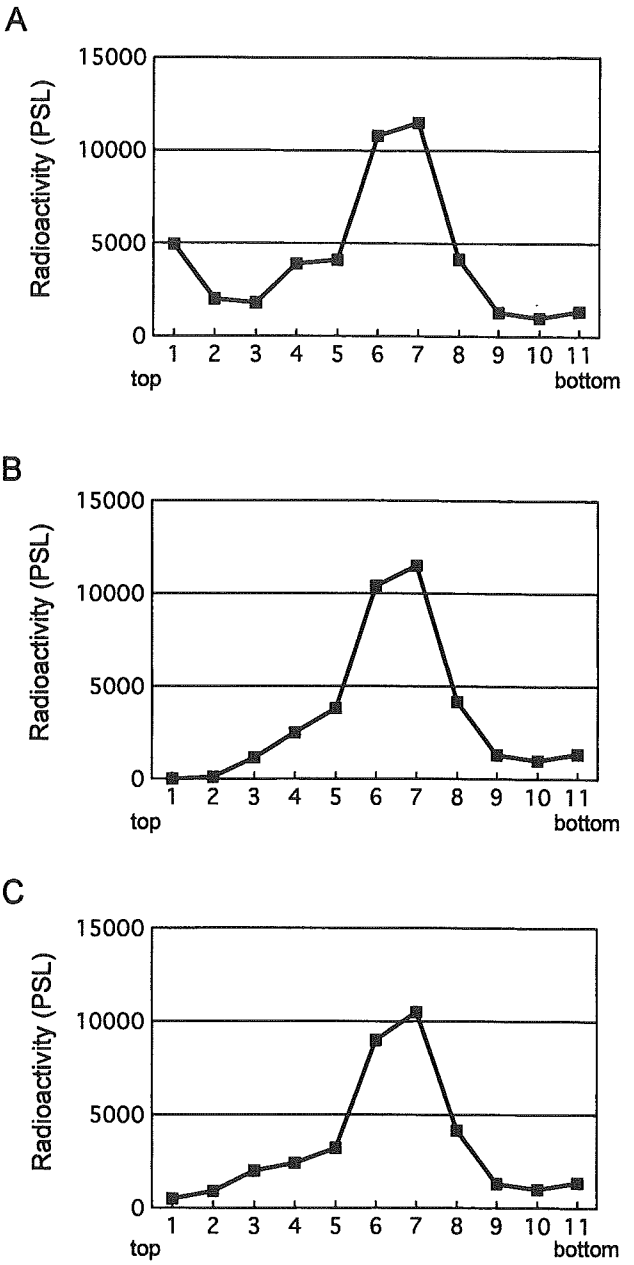

Fig. 1. Sedimentation profiles of viral N antigens separated from infected cell lysates in a sucrose density gradient. Rabies virus infected cells were metabolically labeled with L-[^{35}S]methionine for 6 hr from 40 to 46 hr after the infection. Then the cells were lysed in a DOC-free RIPA(I) buffer, followed by clarification by high speed centrifugation (5,000 rpm, 5 min). The lysates were applied to a 10–40% sucrose density gradient. After ultracentrifugation for 2 hr at 25,000 rpm, the gradient was divided into 10 fractions and the bottom fraction (pellet). Each fraction was subjected to immunoprecipitation with anti-N pAb (A) and mAbs #404-11 (B) and #1-7-11 (C), and then applied to procedures for SDS-PAGE and autoradiographic analysis in a Bio-Imaging Analyzer BAS2000. Radioactivity (PSL) of the N protein band was determined for all fractions and plotted in a graph for each antibody.

50 mM Tris-HCl, 1 mM pefabloc, and 25 μg/ml leupeptin, pH 7.4). After brief centrifugation [10 min at 5,000 rpm (≒5,000×*g*)] in a microfuge, the lysates were applied to ultra-centrifugation at 46,000 rpm (200,000×*g*) for 2 hr through a 20% sucrose cushion. The NC pellet was subjected to treatment with alkaline phosphatase as described previously (22). In brief, the pellet was lysed in an alkaline buffer (pH 9.0) containing 1% NP-40, and divided into two equal parts. One half was treated with 25 U alkaline phosphatase of calf intestine (CIAP) for 60 min at 37 C, and another half was mock-treated. Samples were then subjected to immunoprecipitation study with anti-N antibodies.

Immunoprecipitation and autoradiography. Radiolabeled cell lysates (10–20 μl) of the lysates were mixed with 1 to 2 μl of antibody solution and placed on ice for 2 hr, followed by precipitation with Pansorbin cells (a commercial product of insoluble protein A of *Staphylococcus aureus*; Calbiochem) for 2 hr at 4 C. In the case of precipitation with the murine antibodies, precipitates were recovered with the help of rabbit antibody against the murine immunoglobulin for efficient recovery with the Pansorbin cells. The antigen-antibody complexes with Pansorbin cells were then recovered by centrifugation at 12,000 rpm (10,000×*g*), and the immunoprecipitates were dissolved in SDS-PAGE sample lysis buffer and applied to 10% SDS-PAGE (see below). After electrophoresis, the gel was dried onto 3MM filter paper (Whatman), and then exposed to an imaging plate for autoradiographic analysis in a BAS2000 Image Analyzer (Fuji Photograph Film, Co., Ltd.).

SDS-PAGE. Assay samples were dissolved in sample lysis buffer for SDS-PAGE (composed of: 125 mM Tris-HCl, 4.6% SDS, 10% 2-mercaptoethanol, 0.005% bromophenol blue and 20% glycerol; pH 6.8) and applied to 10% polyacrylamide gels prepared by using a discontinuous buffer system. After the electrophoresis, protein bands were subjected to immunoblot analysis (see below) or simply stained with Coomassie Brilliant Blue R-250 (CBB; Merck), and dried onto filter paper for autoradiographic analysis.

Immunoblot analysis. Cell lysates were applied to 10% SDS-PAGE and proteins separated on the SDS-PAGE gels were electrically blotted to nitrocellulose filter using a semi-dry blotting apparatus. After blocking procedures, filters were incubated with the anti-N antibody, and then with the peroxidase-conjugated second antibody. The color was developed by adding H_2O_2 and chloronaphtol. Apparent molecular weight of the proteins was estimated by co-electrophoresis of "Dr. Western" (Oriental Yeast Co.).

Results

Conformation-Dependent Exposure of a Linear Epitope 404-11 of N Protein

We first investigated the epitope specificity of some anti-N mAbs. Metabolically radiolabeled infected cells were lysed in RIPA(I) buffer (DOC-free), and subjected

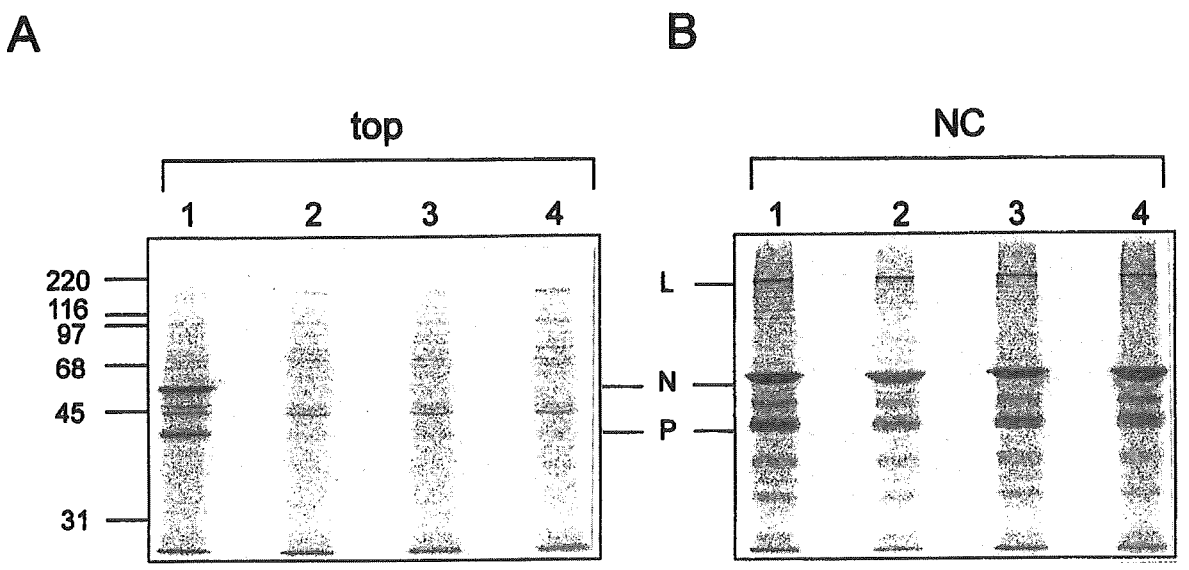

Fig. 2. Antigenic specificity of N proteins in the soluble and NC fractions. Rabies virus infected BHK-21 cells were radiolabeled in a similar manner as described in Fig. 1, and lysed in RIPA(I) buffer, followed by ultracentrifugation to separate them into the soluble (top) and the NC (pellet) fractions as described in "Materials and Methods." Both fractions were subjected to immunoprecipitation with anti-N pAb (lane 1) or mAb #404-11 (lane 2), #1-7-11 (lane 3) or #5-2-26 (lane 4), followed by autoradiographic analysis in a Bio-Imaging Analyzer BAS2000. (A) Soluble fraction. (B) NC fraction.

to ultracentrifugation through a 10–40% sucrose gradient. Then, the gradient was fractionated into ten fractions and also a bottom fraction (fraction #11; dissolved in 0.5 ml RIPA(I) buffer). Each fraction was subjected to immunoprecipitation with either anti-N pAb or anti-N mAb #404-11 or #1-7-11 as described in "Materials and Methods." Then, the precipitates were subjected to 10% SDS-PAGE, which was processed for the autoradiographic analysis in a Bio-Imaging Analyzer BAS2000. Radioactivity of each N protein band was measured for all fractions and plotted to graphs as shown in Fig. 1. Fractions #6 and #7 correspond to the NC fraction (14). We could observe little difference in the sedimentation pattern of N protein recognized by the two mAbs (Fig. 1, B and C). Both mAbs precipitated little N protein from the top fraction which contained the RNA-free N-P complex that could be detected by anti-N pAb (Fig. 1A), suggesting that the epitope structures for the mAbs are not exposed or formed on the RNA-free N protein.

Figure 2 also shows that there is no significant difference among the precipitates recovered with any of three anti-N mAbs from either the RNA-free N-P complex fraction (top fraction; panel A) or the NC fraction (panel B). As shown in lane 1 of panel A, only anti-N pAb precipitated N and P proteins from the N-P complex fraction, but almost no precipitates were obtained by any of three mAbs, #1-7-11, #5-2-26 and #404-11 (lanes 2, 3 and 4 of panel A).

In this experiment, we noticed that when the cells were lysed by a DOC-containing lysis buffer, the precipitates with mAb #404-11 were much smaller in amount. This result was not changed even when the incubation period was prolonged to 4 hr nor by increasing the amount of the mAb by fourfold for the immunoprecipitation (data not shown). This point was further examined more precisely using the isolated NC. As expected, the amount of N protein recovered by mAb #404-11, but not by other mAbs, was greatly reduced (Fig. 3). In this experiment, P and L proteins were mostly dissociated from the NC (see lanes 2 and 6). From these results, it is suggested that the epitope site is concealed by conformational change after the removal of P and/or L proteins by DOC treatment, or by interaction with DOC.

We further examined the effect of dephosphorylation of N protein (removal of phosphate group) on the antigenicity to these mAbs. CIAP-treated NC fraction was subjected to immunoprecipitation with these mAbs. As shown in Fig. 4, antigenicity to mAb #404-11, but not #1-7-11, was greatly reduced (compare the lanes 4 and 6). In this experiment, it was also noticed that the content of NC-associated P proteins, but not so much of the L protein, was greatly reduced by phosphatase-treatment (lanes 2 and 6) as described in our previous study (23). From these results, we assume that, although the 404-11 epitope is linear and was independent of N protein phosphorylation (13), it is exposed only when the N protein encapsidate the viral RNA, while the phosphate group on Ser-389 seems to be necessary not only for

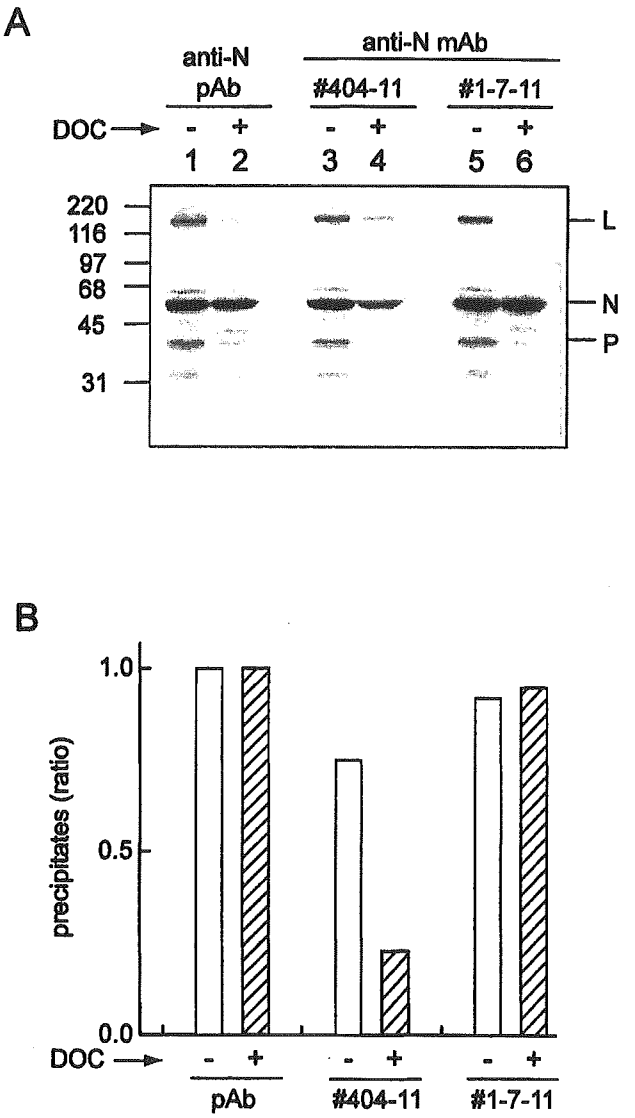

Fig. 3. Effect of DOC on the exposure of 404-11 epitope region of N protein. (A) Rabies virus infected BHK-21 cells were metabolically radiolabeled as described in Fig. 1, and lysed in DOC-free RIPA(I) or 1% DOC-containing RIPA(II) buffer, and then ultracentrifugated at 46,000 rpm for 2 hr at 4 C. The NC-containing pellets were recovered and subjected to immunoprecipitation with anti-N pAb (lanes 1 and 2) and mAbs #404-11 (lanes 3 and 4) and #1-7-11 (lanes 5 and 6). Lanes 1, 3 and 5: untreated control; lanes 2, 4 and 6: DOC-treated. (B) Radioactivity of the N protein band shown in panel A was determined in a Bio-Imaging Analyzer BAS 2000 for each lane and depicted in a bar graph as a ratio to that of the control which was recovered by anti-N pAb from the whole cell lysates prepared in a DOC-free RIPA(I) buffer.

keeping the P protein association, but also for keeping the 404-11 epitope-positive conformation.

There seems to also be a positive relationship between the content of NC-associated P proteins and the antigenicity to mAb #404-11. Further, the amount of NC-associated L protein was apparently proportional to the amount of NC-associated P protein, or to that of the NC-associated phosphorylated form of P protein, but probably not to the amount of 404-11 epitope-positive NC (also see "Discussion").

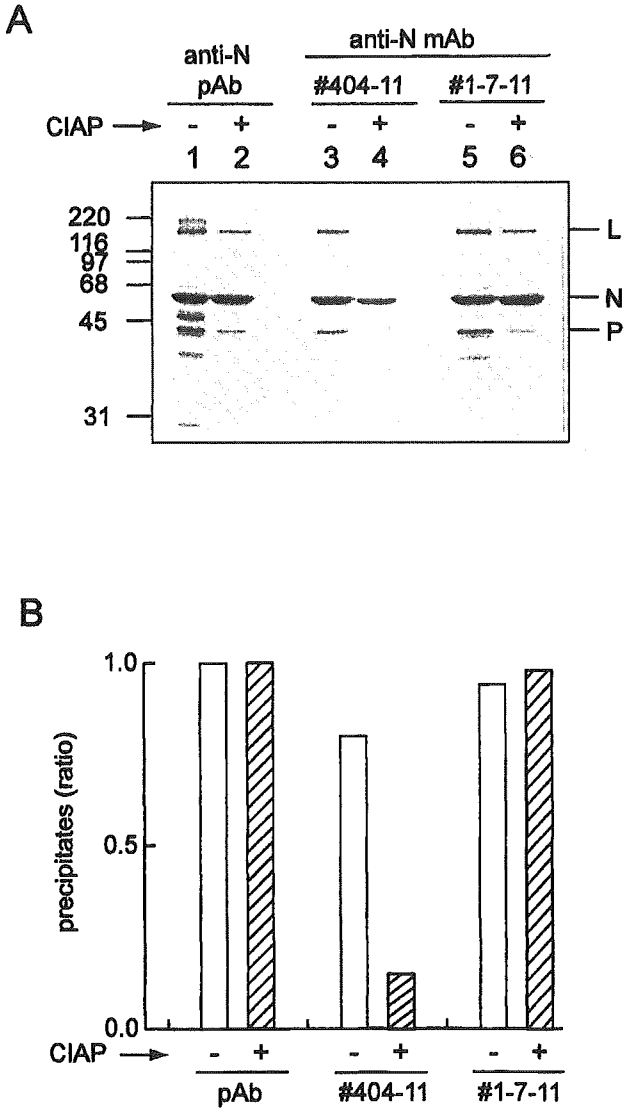

Fig. 4. Effect of deprivation of phosphate group from the NC on the antigenicity of N protein to mAb #404-11. (A) Infected cells were radiolabeled and lysed as described in Fig. 1, and ultracentrifuged to recover the NC fraction in pellets. They were resuspended in 1% NP-40-containing alkaline phosphatase buffer, and divided into two equal parts, one of which was treated with CIAP, and another half was mock-treated. Then, pH of the reaction mixture was lowered to neutral (see "Materials and Methods"), and subjected to the immunoprecipitation with anti-N pAb (lanes 1 and 2), or mAb #404-11 (lanes 3 and 4) or #1-7-11 (lanes 5 and 6), followed by SDS-PAGE and autoradiographic analysis. Lanes 1, 3 and 5: untreated control; lanes 2, 4 and 6: CIAP-treated. (B) Radioactivity of each N protein band shown in panel A was determined in a Bio-Imaging Analyzer BAS2000, and depicted in a bar graph as the ratio to that of the untreated control which was precipitated by anti-N pAb.

Mapping of the 404-11 and 1-7-11 Epitopes

As described above, the 404-11 epitope site seemed to be located at a very busy site on the NC in terms of structural or conformational changes for the N protein functions in viral RNA synthesis. Accordingly, we tried to identity the epitope sites on the viral N protein. For this purpose, we used the N cDNAs of the HEP-Flury and Nishigahara (RC-HL) strains since the latter lacked both epitopes (our unpublished data). The HEP and Nishigahara N cDNAs were expressed in BHK-21 cells with the help of RVV-T7, and after being radiolabeled with L-[^{35}S]methionine, cells were lysed in RIPA (I) buffer and applied to immunoprecipitation using

Fig. 5. Epitope mapping of anti-N mAbs #404-11 and #1-7-11. (A) The antigenicity of the N protein of the HEP-Flury and Nishigahara RC-HL strains was compared. BHK-21 cells were transfected with the N cDNA of the HEP-Flury strain or Nishigahara RC-HL strain with RVV-T7, or mock-transfected, and incubated in the presence of ara-A (10 μg/ml). They were labeled with L-[^{35}S]methionine for 4 hr from 20 hr after the transfection, and then lysed in RIPA(I) buffer and subjected to immunoprecipitation with anti-N pAb (lanes 1, 2 and 3), or mAb #404-11 (lanes 4, 5 and 6) or #1-7-11 (lanes 7, 8 and 9). The precipitates were run in 10% SDS-PAGE gel and then processed for autoradiographic analysis in a Bio-Imaging Analyzer BAS2000. (Samples) Lanes 1, 4 and 7: HEP-Flury strain; lanes 2, 5 and 8: Nishigahara RC-HL strain; lanes 3, 6 and 9: mock. (B) Reactivity to mAb #404-11 was examined for the products of recombined N genes that were reconstructed by cutting and ligation at the *Eco*T22I site of N protein using the N cDNA of the HEP-Flury and Nishigahara RC-HL strains. After the radiolabeling, cDNA-transfected cells were lysed in RIPA (I) buffer and subjected to immunoprecipitation with anti-N pAb (lanes 1, 2 and 3), or mAb #404-11 (lanes 4, 5 and 6) or #1-7-11 (lanes 7, 8 and 9), and processed for autoradiographic analysis in a Bio-Imaging Analyzer BAS2000. (Samples) Lanes 1, 4 and 7: N[HEP/RC-HL (*Eco*T22I)]; lanes 2, 5 and 8: N[RC-HL/HEP (*Eco*T22I)]; lanes 3, 6 and 9: control (no cDNA transfection). (C) Reactivity of the trypsin-cleaved N protein with mAb #404-11 was examined as follows. Rabies virus infected cells were lysed in RIPA(I) buffer at 46 hr after the infection, and ultracentrifuged at 46,000 rpm for 2 hr to recover the NC in pellets, which was resuspended in a RIPA(I) buffer, and then divided into three equal parts. They were treated with trypsin at a concentration of 2.5 μg/ml (lanes 1 and 4) or 0.5 μg/ml (lanes 2 and 5) or mock-treated (lanes 3 and 6) for 1 hr at 37 C, followed by dissolving in SDS-PAGE sample buffer. Then, they were processed for immunoblotting with anti-N pAb (lanes 1, 2 and 3) and mAb #404-11 (lanes 4, 5 and 6).

mAbs #404-11 and #1-7-11 as well as anti-N pAb. As shown in Fig. 5A, both mAbs did not recognize the Nishigahara virus N protein.

We next examined the antigenicity of recombined N cDNAs that were prepared by exchanging the counterparts of N cDNAs of two rabies virus strains cut at the same restriction site (e.g., *Eco*T22I or *Sty*I site; 7; also see Fig. 6). They were similarly expressed in BHK-21

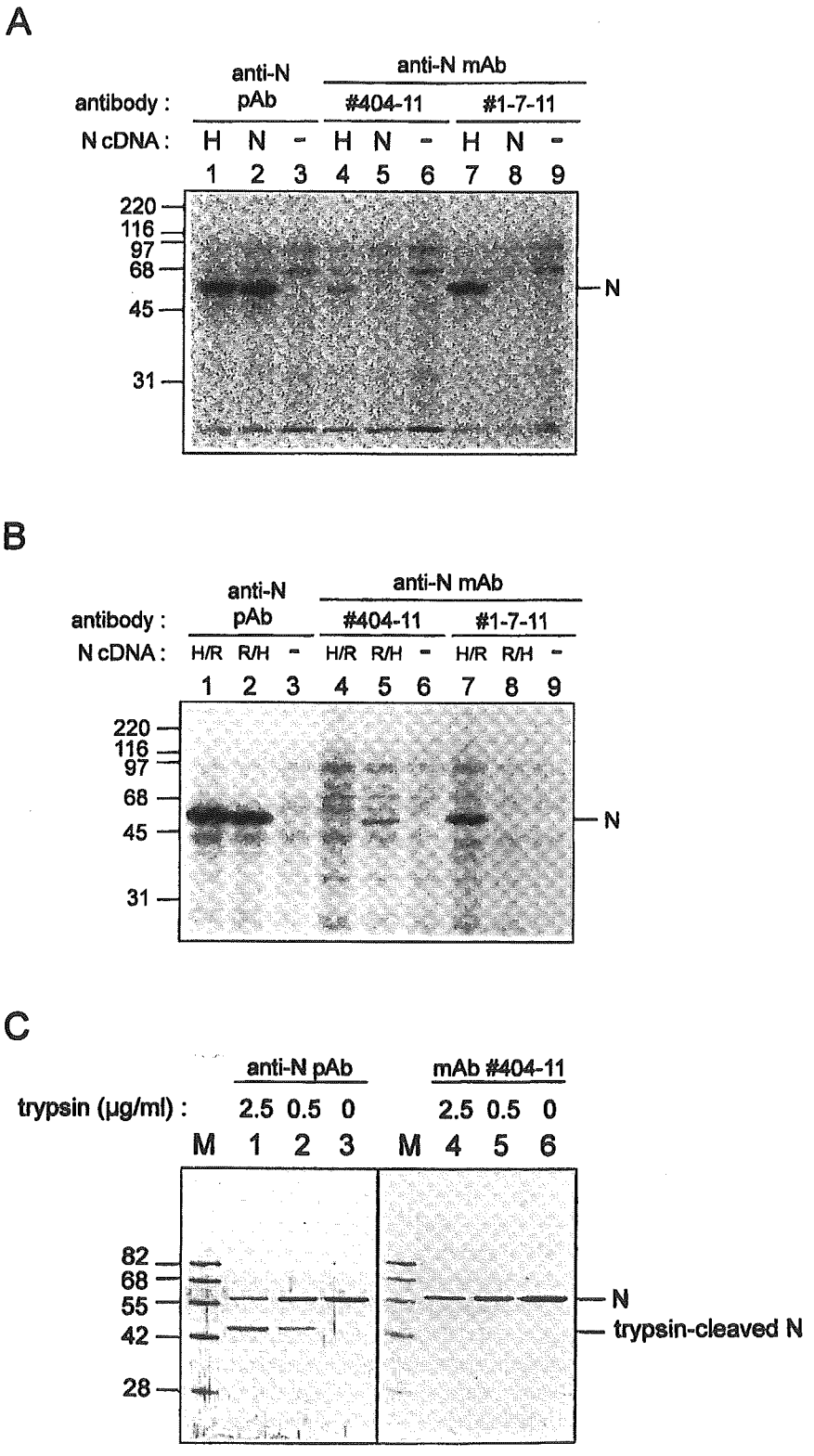

Fig. 5.

cells and subjected to immunoprecipitation using anti-N mAbs. As shown in Fig. 5B, immunoprecipitation studies with the recombinant N proteins showed that, if the N-terminal side of HEP N cDNA cut at the *Eco*T22I site is exchanged with that of Nishigahara, the antigenicity to mAb #1-7-11 was lost, while that to #404-11 was preserved (compare lanes 5 and 8). On the other hand, if the C-terminal side of HEP-N cDNA was replaced by that of the Nishigahara strain, the antigenicity to mAb #404-11 was lost, but that to #1-7-11 was preserved (compare lanes 4 and 7). From these observations, we assume that the 404-11 epitope is located on the C-terminal side, while the N-terminal fragment is involved in the 1-7-11 epitope formation. Studies with other recombinants prepared by cutting and recombining at the *Sty*I site demonstrated that a small N-terminal fragment composed of the first to 42nd amino acids contains a specific region that is essential for forming the 1-7-11 epitope (Fig. 6).

For further mapping the 404-11 epitope, we used C-terminal deletion mutants that were prepared by inserting a stop codon-containing *Nhe*I linker at some restric-

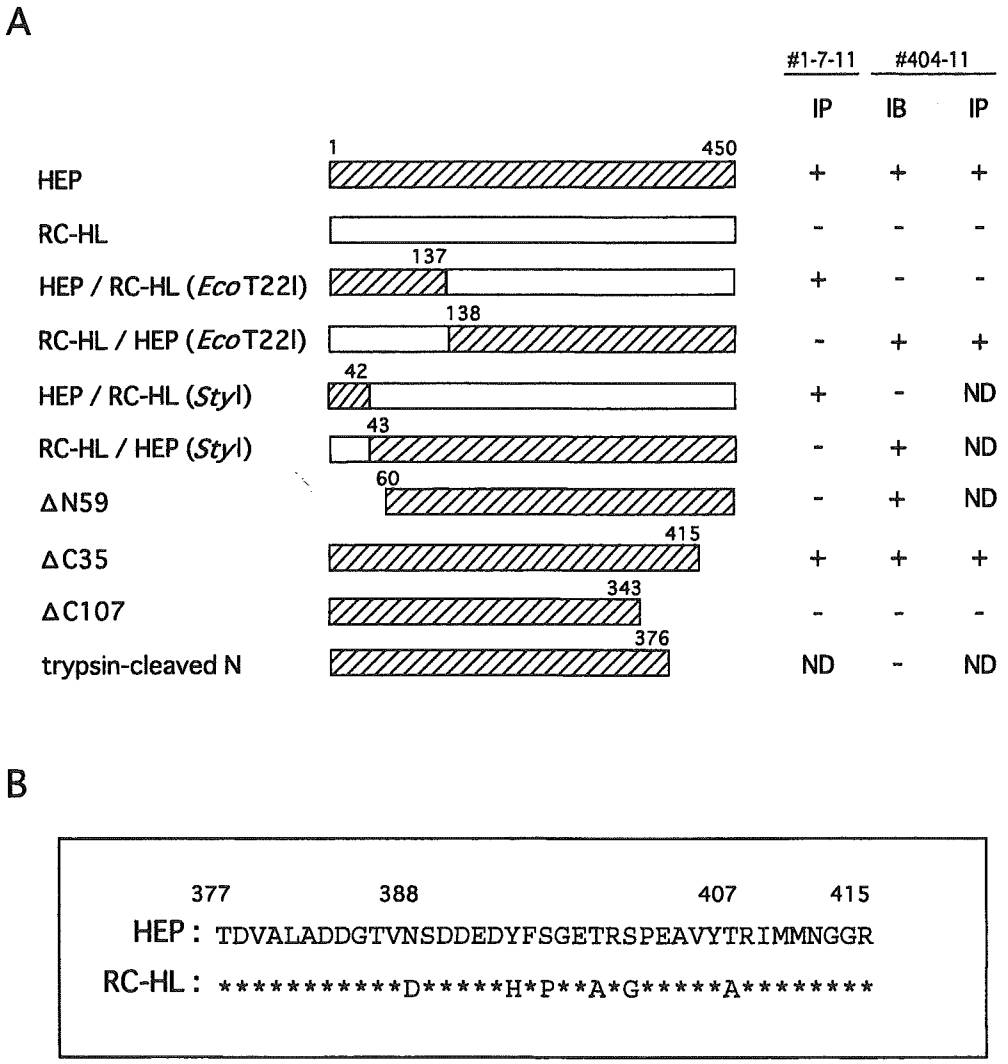

Fig. 6. Epitope mapping of mAbs #404-11 and #1-7-11. (A) Schematic illustration of the structures of recombined N proteins and deletion mutants and their antigenicity to anti-N mAbs. Recombined N proteins and the deletion mutants produced in the cDNA-transfected cells were lysed in SDS-PAGE sample buffer and subjected to immunoblotting with mAb #404-11, or metabolically radiolabeled and then subjected to the immunoprecipitation with anti-N mAbs #1-7-11 and #404-11. Results shown in Fig. 5 were also summarized in this figure combined with other data for deletion mutants (data not shown) also, and depicted to the right. IP: immunoprecipitation with mAb #404-11 or #1-7-11; IB: immunoblotting with mAb #404-11. (B) Comparison of amino acid sequence in a postulated 404-11 epitope-containing fragment of the N protein (amino acid positions from 377 to 415) between the HEP-Flury (upper) and Nishigahara RC-HL strain (bottom). Identical amino acids are depicted in asterisks, and only non-identicals are depicted for the RC-HL strain.

tion sites as described previously (1). In studies with these deletion mutants, the 404-11 epitope could be mapped to a region ranging from 343 to 415 amino acids (Fig. 6A). Furthermore, the trypsin-digested N protein, which is known to be deprived of the C-terminal 74 amino acids (15), was recognized by mAb #404-11 (Fig. 5C). From these results, we assume that the 404-11 epitope site is located in a region ranging from 377 to 415 amino acids. In such a region, we could find six non-identical amino acids when the amino acid sequence of the HEP and Nishigahara (RC-HL) stains were compared (Fig. 6B), which are located in a small region from amino acid positions 388 to 407. Accordingly, we can conclude that the 404-11 epitope is mapped to a narrow region around the amino acid positions 388 to 407. In this study, we also noticed that a C-terminal deletion mutant (ΔC107) was not recognized by mAb #1-7-11, while another mutant (ΔC35) was recognized by the mAb, implicating that a certain C-terminal region is also involved in some way in the 1-7-

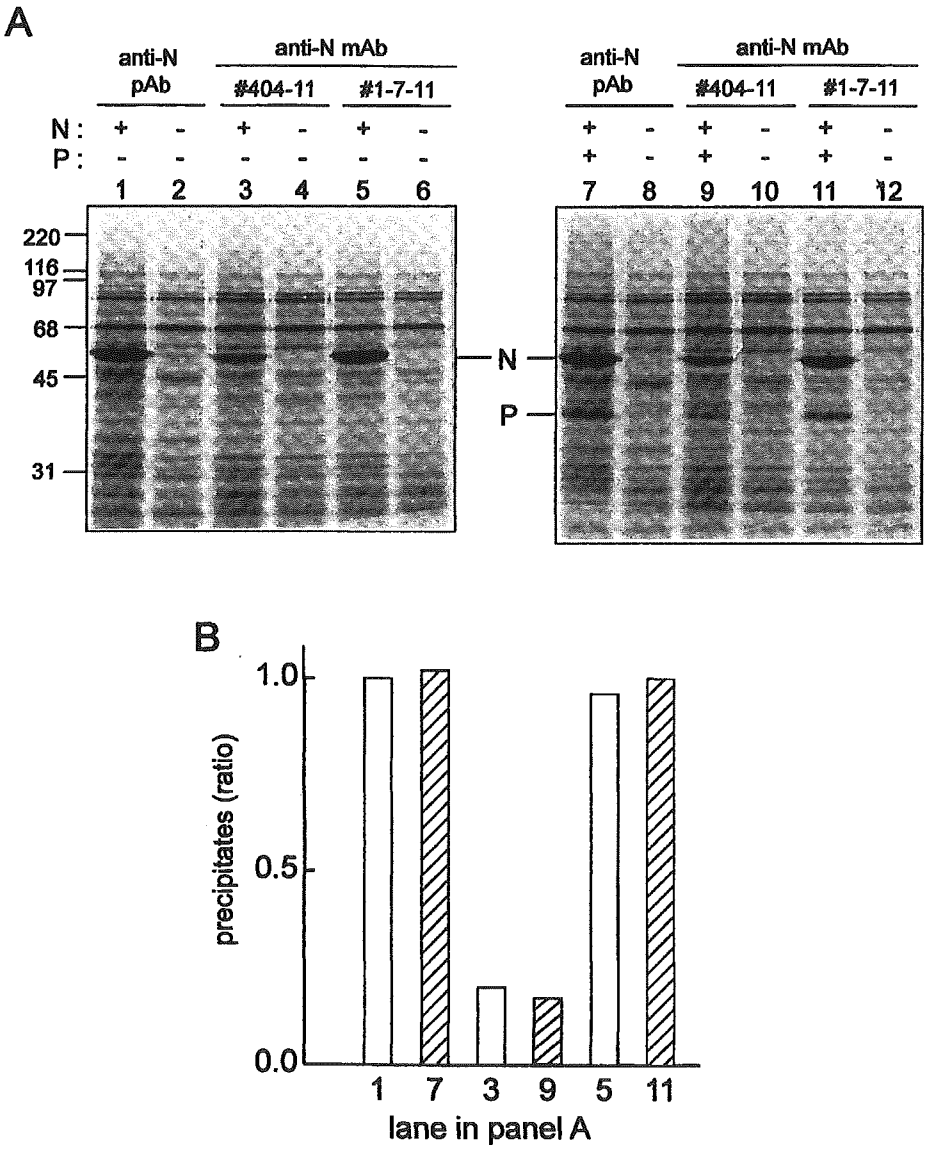

Fig. 7. Examination of the effect of P protein co-expression on the antigenic maturation of N protein. (A) BHK-21 cells were transfected with the N cDNA alone or co-transfected with both the N and P cDNAs with the help of RVV-T7. Mock-transfection was done without the cDNA but with RVV-T7. Metabolic radiolabeling was performed as described in Fig. 5A. Then, they were lysed in RIPA(I) buffer and subjected to immunoprecipitation with anti-N pAb (lanes 1, 2, 7 and 8) and mAbs #404-11 (lanes 3, 4, 9 and 10) and #1-7-11 (lanes 5, 6, 11 and 12), followed by SDS-PAGE and autoradiographic analysis as described in "Materials and Methods." Lanes 1, 3 and 5: N cDNA alone; lanes 7, 9 and 11: (N+P) cDNAs; lanes 2, 4, 6, 8, 10 and 12: mock-transfected (RVV-T7 alone). (B) Radioactivity of the N protein band of each lane was determined in a Bio-Imaging Analyzer BAS2000, and plotted in a bar graph as a ratio to that of the sample of N cDNA alone recovered with anti-N pAb (lane 1).

11 epitope formation.

Studies on the NC-Like Structure Produced in the N cDNA-Transfected Cells

During the epitope study, we noticed that the N proteins produced in the N cDNA-transfected cells (composing the NC-like structure; 14) were not efficiently recognized by mAb #404-11 (Fig. 5A, lane 4). This point was further investigated more precisely. The left panel (lanes 3 to 6) of Fig. 7 compares the different recognition efficiency displayed by two anti-N mAbs #404-11 and #1-7-11 against the NC-like structure produced in the N cDNA-transfected BHK-21 cells. MAb #1-7-11 recognized the NC-like structure as efficiently as anti-N pAb, while mAb #404-11 did not, implicating that most N proteins took the NC-like structure probably with nonspecific RNAs (i.e., they are assembled with non-viral RNAs to form NC-like structures, phosphorylated at Ser-389, and taking the NC-like conformation; 14, 16). Such NC-like structures, however, were much less efficiently recognized by mAb #404-11 (Fig. 7, lane 3). Such a low efficiency was not improved at all by co-expression with the viral P protein as shown in the right panel (lanes 9 to 12) of Fig. 7. Furthermore, co-expression of N and M proteins did not result in increasing the 404-11 epitope formation on the N protein (data not shown).

Due to this, we next examined the effect of co-expression of the minigenome RNA whose 3′- and 5′-end was derived from the viral genomic structure. This RNA could be expected to be assembled with the N-P complexes to form a ribonucleoprotein (RNP)-like structure. As shown in Fig. 8, co-expression of N and P cDNAs with the minigenomic RNA resulted in significantly enhanced reactivity of the NC/RNP-like structures with mAb #404-11, while the co-expression without the P protein did not.

Discussion

Epitope mapping. We investigated conformational changes of the rabies virus nucleocapsid (N) protein which could be detected by its different reactivity to anti-N mAbs #1-7-11 and #404-11. For this purpose, we also tried to map the epitope sites on the N protein. At the least, an N-terminal fragment of 42 amino acids was suggested to be responsible for the conformational 1-7-11 epitope formation. Studies with deletion mutants suggested that a C-terminal sequence, ranging from amino acid positions 344 to 415, also contained a region that was necessary to form the 1-7-11 epitope. On the other hand, a linear 404-11 epitope was mapped to a small region that was composed of amino acid positions from 388 to 407, in which a regular phosphorylation site (Ser-389; 1) is located.

In our previous study (14), we showed that the P protein deprivation from the NC did not affect the exposure of 5-2-26 epitope site on the N protein. On the other hand, the 404-11 epitope region was concealed again

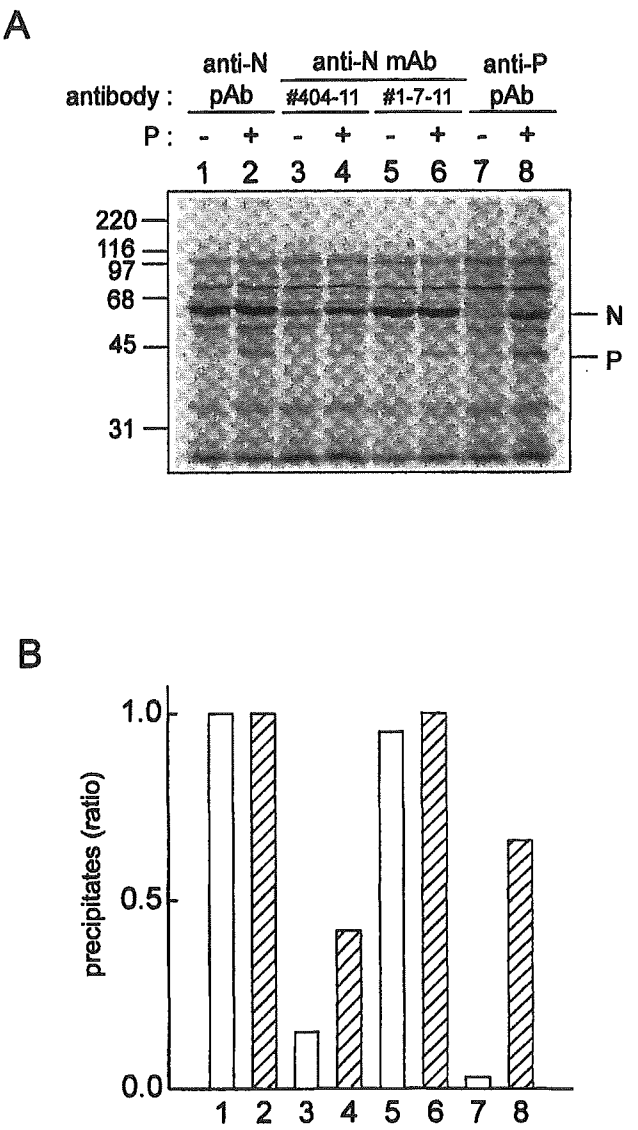

Fig. 8. Enhanced reactivity of the NC/RNP-like structures to mAb #404-11 when co-transfected with the minigenome. (A) BHK-21 cells were transfected with the N cDNA and a cDNA encoding the minigenome with or without the P cDNA. They were radiolabeled as described in Fig. 5A, they were lysed in a DOC-free RIPA(I) buffer and subjected to immunoprecipitation with anti-N pAb (lanes 1 and 2) or mAb #404-11 (lanes 3 and 4) or #1-7-11 (lanes 5 and 6). P protein production was checked also by immunoprecipitation with anti-P pAb (lanes 7 and 8). (B) Radioactivity of the N protein band was determined for each lane in a Bio-Imaging Analyzer BAS2000, and depicted in a bar graph as a ratio to that of the precipitates obtained with anti-N pAb from the "N+minigenome (without P protein)" sample shown on lane 1.

when the P protein was removed from the NC by DOC treatment. From these observations, we assume that Ser-389 is not included in the 404-11 epitope site. In addition, both the 5-2-26 and 404-11 epitope regions are concealed inside the N protein molecule when the N protein is present in a free form of RNA-free N-P complex (14). Based on these considerations, we think that the 404-11 epitope site is located in a little downstream region from the Ser-389 (see possible functional and epitope mappings shown in Fig. 9).

The 5-2-26 and 404-11 epitope sites are located 40–50 amino acids downstream from the direct RNA-binding domain which was identified by Kouznetzoff et al. (15). In addition, deletion of C-terminal 45 amino acids from the N protein was shown to abrogate the RNA-binding ability of N protein (25). Our present data, however, showed that the C-terminal 35 amino acids are not essential for the N protein to display the RNA-binding activity because the conformational 1-7-11 epitope is formed by a C-terminal deletion mutant (NΔC35) of N protein that lacked 35 amino acids from the C-terminal (the 1-7-11 epitope is formed only when the N protein encapsidates the viral RNA; 14). Accordingly, the C-terminal region which is additionally required for displaying the RNA-binding activity may partly overlap the 404-11 epitope-containing region (Fig. 9).

Conditions for exposing the 404-11 epitope region. Although the 404-11 epitope is a linear one, it was not detected on the N protein of RNA-free N-P complex. The epitope was detected on the NC/RNP, suggesting that the 404-11 epitope region was enclosed inside the N-P complex and was exposed after encapsidation of viral RNA. The epitope site is concealed again when

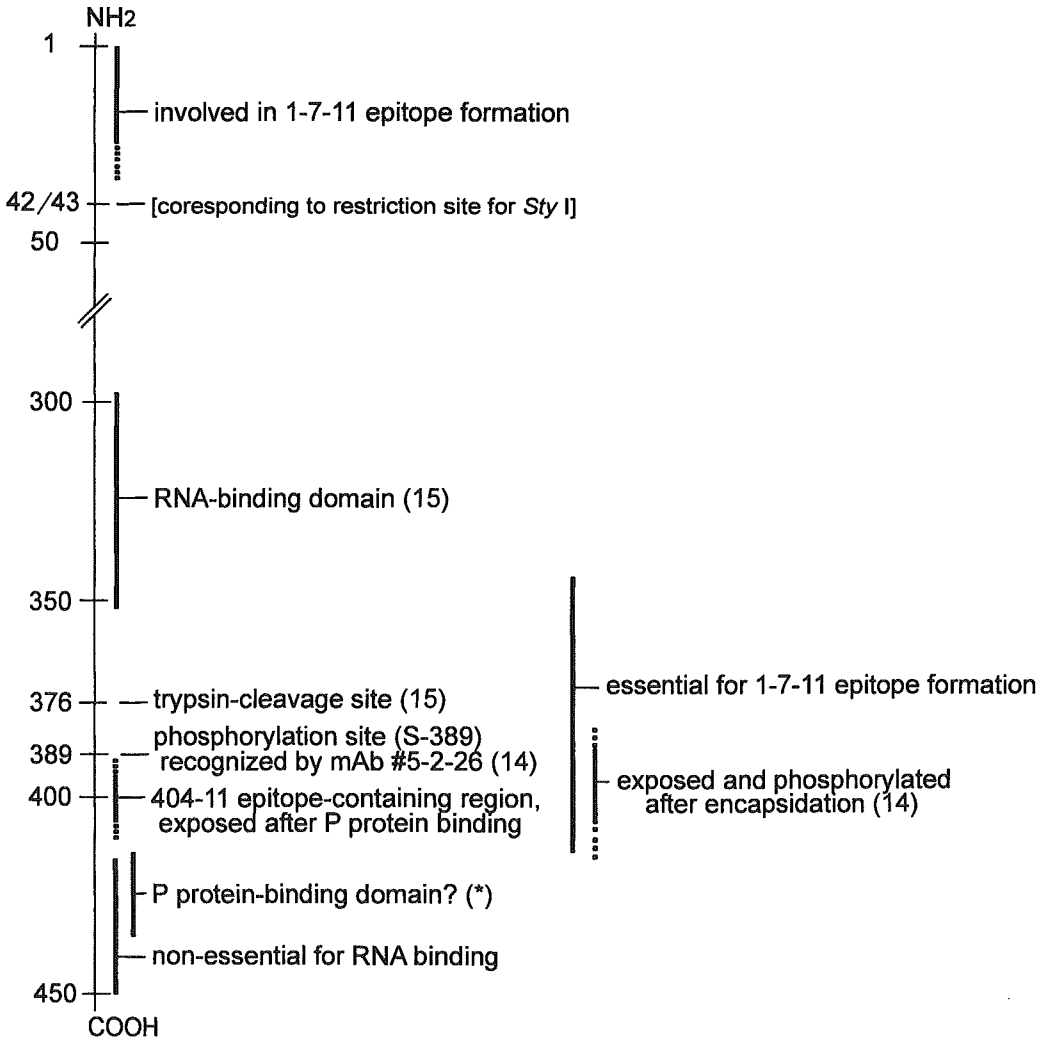

Fig. 9. Schematic illustration for the summary of mapping of the functional domains and epitope-related regions recognized by some anti-N mAbs (see the text). *: P protein-binding domain was deduced from a report by Iseni et al. (9), describing that the domain was cleaved off from the N protein by trypsin digestion. In this study, it was shown that a region comprised of amino acids 390 to 407 is exposed after the P protein binding.

the NC/RNP was deprived of P proteins by treatment with CIAP or DOC. In our previous study, it was suggested that the N protein phosphorylation was necessary to keep the P protein association with the NC and NC-like structures (23). In our present study, we further showed that removal of P proteins from the NC by treatment with CIAP or DOC reduced its antigenicity to mAb #404-11, but not to #1-7-11. Further, we assume that the NC-associated P protein is necessary to keep the 404-11 epitope-positive conformation, and that the reduced antigenicity to mAb #404-11 seen after the CIAP treatment is due rather to removal of P proteins from the NC. We think that, if P proteins are dissociated from the NC, such 404-11 epitope-positive conformation would become unstable, and might be converted to the 404-11 epitope-negative (or, concealed) form. Based on these considerations, we assume that the 404-11 epitope is exposed only after the encapsidation of the viral RNA, and the 404-11 epitope-positive conformation is stabilized both by phosphorylation at Ser-389 (23) and by re-association with the P protein of altered conformation (a form that is recognized by anti-P mAb #402-13; 21), probably for receiving the L protein or for the packaging into the virion (see below).

Multiple conformations of N protein. The N protein may take one of three or four different structures and/or conformations, including the RNA-free N-P complex, intracellular newly synthesized NC and template-active NC in viral RNA synthesis as well as the NC packed in the virion (Table 2). In our previous study, we observed that the N protein changes its molecular structure at the step of encapsidation of viral RNA in terms of conformational epitopes formation, which could be recognized by acquisition of its reactivity to several anti-N mAbs (#5-2-26, #1-7-11, etc.; 14). The N protein may additionally perform minor changes in the conformation after encapsidation of genomic RNA and phosphorylation at Ser-389 (Table 2). Present studies suggest strongly that, after the viral RNA encapsidation, the NC proteins additionally change their conformation probably depending on the tasks given to it in the cell, which could be recognized by absence or presence of the antigenicity to mAb #404-11. Such changes of NC might be controlled by association and dissociation of the viral P protein (Table 2).

The P protein-binding site on the NC was suggested

Table 2. Antigenic structures of N protein under various conditions

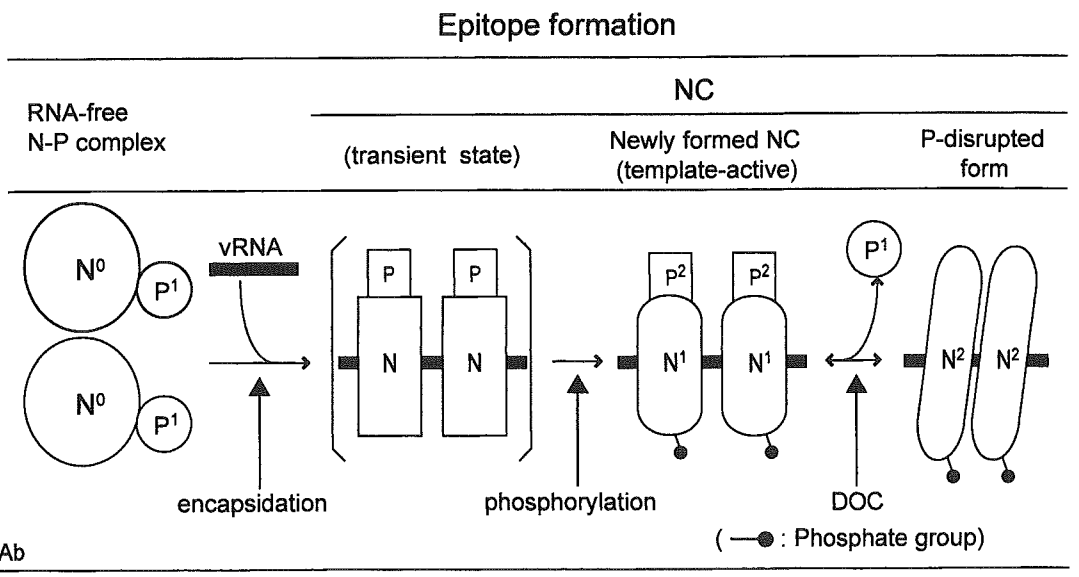

Both N and P proteins undergo conformational changes during and/or after encapsidation of viral genome-sized RNA. After encapsidation, the N protein could be recognized by mAbs #1-7-11, #5-2-26 and #404-11, but recognition by mAb #5-2-26 is dependent on the phosphorylation at Ser-389 of N protein. After dissociation of P proteins from the NC by DOC-treatment, the N protein could not be recognized by mAb #404-11. N^0: non-phosphorylated form of N protein; N^1: NC-forming N protein (P protein-associated form); N^2: NC-forming N protein (without P protein association). P^1: 402-13 epitope-negative form of P protein; P^2: 402-13 epitope-positive form of P protein (21).

to be located in a C-terminal small region of N protein which could be cut off at Lys-376 by trypsin digestion (19). Since disclosure and enclosure of 404-11 epitope-containing region was suggested to be dependent on the association and dissociation of P protein, we further speculate that the 404-11 epitope-containing region is involved in a certain activity or activities of viral NC in collaboration with the P protein, such as its template activity for viral RNA synthesis and/or accessibility of the viral RNA polymerase (L protein) to the NC, or initiation of the NC-packaging into the virion.

Studies using the N cDNA expression system. Expression of N protein either with or without co-expression of P protein in animal cells has been known to produce the NC-like structures which resemble the viral NC that is produced in the infected mammalian cells in terms of their morphology visualized by electron microscopy and other specific points including the antigenicity to conformational epitope-specific mAbs (9, 14, 19, 25). Our present study, however, suggested that the NC-like structures produced in the N cDNA-transfected BHK-21 cells were somewhat different in their higher structure from the viral NCs produced in the infected cells. For instance, they were recognized very efficiently by most of our anti-N mAbs (14), except for a linear epitope-specific mAb #404-11, which recognized very weakly the NC-like structures. This means that the 404-11 epitope-containing region (amino acid positions 390 to 407; Fig. 9) is concealed inside the NC-like structure, while the neighboring phosphorylation site at Ser-389 is exposed as revealed by its reactivity to anti-N mAb #5-2-26 (1, 14). Further, co-expression of the P protein was not helpful for the N protein to expose the 404-11 epitope region. However, the co-expression of the minigenomic RNA resulted in significantly enhanced reactivity of the NC/RNP-like structures to mAb #404-11 (Fig. 8), suggesting strongly that the antigenic maturation of N protein is dependent on the normal assembly with the genomic (and antigenomic) RNA. In this study, however, the amount of 404-11 epitope-positive NC/RNP-like structures was not so large as the NC/RNP-like structures that were recovered by mAb #1-7-11, probably due to still inefficient usage of the N-P complexes for the encapsidation of minigenomic RNA, when compared with the nonspecific encapsidation of nonviral RNAs.

Normal assembly of the viral RNA with specific N proteins might be essential for the RNA to work as the template in viral RNA synthesis and/or to bud out from the plasma membrane forming the progeny virion. Yang et al. (25) described that the (+)-strand leader RNA transcript contained a specific initiation signal for the leader RNA encapsidation by N proteins. In addition, the RNA encapsidation process is performed with the help of the P protein which works as the molecular chaperone to the N protein preventing the assembly with nonspecific RNAs (16). Taking our results obtained with the minigenomic RNA (Fig. 8) and a report by Yang et al. (25) together into consideration, we assume that N proteins achieve final antigenic maturation after the encapsidation, including conformational changes to expose its 404-11 epitope-containing region. To achieve this process completely, the N protein should first recognize a presumed signal or motif located in transcripts of the leader as well as the trailer regions probably assuring the initiation of specific RNA encapsidation by the N protein. In addition, conformational changes of the N protein might be regulated even after the RNA encapsidation probably by dissociation and reassociation of the P protein on the RNP, which might be essential for the RNP to function as the template in viral RNA synthesis.

Sincere gratitude is due to Dr. Nobuyuki Minamoto (Gifu University) for his kind donation of a cDNA clone of the Nishigahara strain nucleoprotein and its recombinant cDNAs. We are grateful to Dr. Tadafumi S. Tochikura for his great efforts in critical reading of the manuscript and to Miss Ai Matsumura for her assistance in manuscript preparation. This work was supported in part by Grants-in-Aid for Scientific Research (No. 11670293 and No. 14570262) from the Ministry of Education, Culture Sports, Science and Technology, Japan.

References

1) Anzai, J., Takamatsu, F., Takeuchi, K., Kohno, T., Morimoto, K., Goto, H., Minamoto, N., and Kawai, A. 1997. Identification of a phosphatase-sensitive epitope of rabies virus nucleoprotein which is recognized by a monoclonal antibody 5-2-26. Microbiol. Immunol. **41**: 229–240.
2) Chen, C., and Okayama, H. 1987. High-efficiency transformation of mammalian cells by plasmid DNA. Mol. Cell. Biol. **7**: 2745–2752.
3) Chenik, M., Chebli, K., Gaudin, Y., and Blondel, D. 1994. *In vivo* interaction of rabies virus phosphoprotein (P) and nucleoprotein (N): existence of two N-binding sites on P protein. J. Gen. Virol. **75**: 2889–2896.
4) Dietzschold, B., Lafon, M., Wang, H., Otvos, L., Celis, E., Wunner, W.H., and Koprowski, H. 1987. Localization and immunological characterization of antigenic domains of rabies virus internal N and NS proteins. Virus Res. **8**: 103–125.
5) Fu, Z.F., Zheng, Y., Wunner, W., Koprowski, H., and Dietzschold, B. 1994. Both the N- and the C-terminal domains of the nominal phosphoprotein of rabies virus are involved in binding to the nucleoprotein. Virology **200**: 590–597.
6) Goto, H., Minamoto, N., Ito, H., Sugiyama, M., Kinjyo, T., Mannen, K., Mifune, K., and Kawai, A. 1994. Nucleotide sequence of the nucleoprotein gene of the RC-HL strain of rabies virus, a seed strain used for animal vaccine produc-

tion in Japan. Virus Genes **8**: 91–97.
7) Goto, H., Minamoto, N., Ito, H., Luo, T.R., Sugiyama, M., Kinjyo, T., and Kawai, A. 1995. Express of the nucleoprotein of rabies virus in *Escherichia coli* and mapping of antigenic sites. Arch. Virol. **140**: 1061–1074.
8) Goto, H., Minamoto, N., Ito, H., Ito, N., Sugiyama, M., Kinjo, T., and Kawai, A. 2000. Mapping of epitopes and structural analysis of antigenic sites in the nucleoprotein of rabies virus. J. Gen. Virol. **81**: 119–127.
9) Iseni, F., Barge, A., Baudin, F., Blondel, D., and Ruigrok, R.W.H. 1998. Characterization of rabies virus nucleocapsids and recombinant nucleocapsid-like structures. J. Gen. Virol. **79**: 2909–2919.
10) Kawai, A., Matsumoto, S., and Tanabe, K. 1975. Characterization of rabies viruses recovered from persistently infected BHK cells. Virology **67**: 520–533.
11) Kawai, A., and Morimoto, K. 1994. Functional aspects of lyssavirus proteins. Curr. Top. Microbiol. Immunol. **187**: 27–42.
12) Kawai, A., and Takeuchi, K. 1992. Temperature-sensitivity of the replication of rabies viruses (HEP-Flury strain) in BHK-21 cells. I. Alteration of viral RNA synthesis at the elevated temperature. Virology **186**: 524–532.
13) Kawai, A., Anzai, J., Honda, Y., Morimoto, K., Takeuchi, K., Kohno, T., Wakisaka, K., Goto, H., and Minamoto, N. 1997. Monoclonal antibody #5-2-26 recognizes the phosphatase-sensitive epitope of rabies virus nucleoprotein. Microbiol. Immunol. **41**: 33–42.
14) Kawai, A., Toriumi, H., Tochikura, T.S., Takahashi, T., Honda, Y., and Morimoto, K. 1999. Nucleocapsid formation and/or subsequent conformational change of rabies virus nucleoprotein (N) is a prerequisite step for acquiring the phosphatase-sensitive epitope of monoclonal antibody 5-2-26. Virology **263**: 395–407.
15) Kouznetzoff, A., Buckle, M., and Tordo, N. 1998. Identification of a region of the rabies virus N protein involved in direct binding to the viral RNA. J. Gen. Virol. **79**: 1005–1013.
16) Liu, P., Yang, J., Wu, X., and Fu, Z.F. 2004. Interactions amongst rabies virus nucleoprotein, phosphoprotein and genomic RNA in virus-infected and transfected cells. J. Gen. Virol. **85**: 3725–3734.
17) Mavrakis, M., Iseni, F., Mazza, C., Schoehn, G., Ebel, C., Gentzel, M., Franz, T., and Ruigrok, R.W.H. 2003. Isolation and characterisation of the rabies virus N^0-P complex produced in insect cells. Virology **305**: 406–414.
18) Minamoto, N., Tanaka, H., Hishida, M., Goto, H., Ito, H., Naruse, S., Yamamoto, K., Sugiyama, M., Kinjo, T., Mannen, K., and Mifune, K. 1994. Linear and conformation-dependent antigenic sites on the nucleoprotein of rabies virus. Microbiol. Immunol. **38**: 449–455.
19) Schoehn, G., Iseni, F., Mavrakis, M., Blondel, D., and Ruigrok, R.W.H. 2001. Structure of recombinant rabies virus nucleoprotein-RNA complex and identification of the phosphoprotein binding site. J. Virol. **75**: 490–498.
20) Takamatsu, F., Asakawa, N., Morimoto, K., Takeuchi, K., Eriguchi, Y., Toriumi, H., and Kawai, A. 1998. Studies on the rabies virus RNA polymerase: 2. Possible relationships between the two forms of the non-catalytic subunit (P protein). Microbiol. Immunol. **42**: 761–771.
21) Toriumi, H., Honda, Y., Morimoto, K., Tochikura, T.S., and Kawai, A. 2002. Structural relationship between nucleocapsid-binding activity of the rabies virus phosphoprotein (P) and exposure of epitope 402-13 located at the C terminus. J. Gen. Virol. **83**: 3035–3043.
22) Toriumi, H., Eriguchi, Y., Takamatsu, F., and Kawai, A. 2004. Further studies on the hyperphosphorylated form (p40) of the rabies virus nominal phosphoprotein (P). Microbiol. Immunol. **48**: 865–874.
23) Toriumi, H., and Kawai, A. 2004. Association of rabies virus nominal phosphoprotein (P) with viral nucleocapsid (NC) is enhanced by phosphorylation of the viral nucleoprotein (N). Microbiol. Immunol. **48**: 399–409.
24) Wunner, W.H. 2002. Rabies virus, p. 23–77. *In* Jackson, A.C., and Wunner, W.H. (eds), Rabies, Academic Press (Elsevier Science Imprint), San Diego.
25) Yang, J., Hooper, D.C., Wunner, W.H., Koprowski, H., Dietzschold, B., and Fu, Z.F. 1998. The specificity of rabies virus RNA encapsidation by nucleoprotein. Virology **242**: 107–117.
26) Yang, J., Koprowski, H., Dietzschold, B., and Fu, Z.F. 1999. Phosphorylation of rabies virus nucleoprotein regulates viral RNA transcription and replication by modulating leader RNA encapsidation. J. Virol. **73**: 1661–1664.

Virus Genes 30:1, 37–48, 2005

Nucleocapsid protein of cell culture-adapted Seoul virus strain 80-39: Analysis of its encoding sequence, expression in yeast and immuno-reactivity

JONAS SCHMIDT,[1] BURKHARD JANDRIG,[2] BORIS KLEMPA,[1,6] KUMIKO YOSHIMATSU,[3] JIRO ARIKAWA,[3] HELGA MEISEL,[1] MATTHIAS NIEDRIG,[4] CHRISTIAN PITRA,[5] DETLEV H. KRÜGER[1] and RAINER ULRICH[1,†,*]

[1]*Institute of Virology, Charité Medical School, Campus Mitte, 10098 Berlin, Germany*
[2]*Max Delbrueck Center for Molecular Medicine, Department of Tumor Genetics, 13092 Berlin, Germany*
[3]*Institute for Animal Experimentation, Graduate School of Medicine, Hokkaido University, Kita-ku, Kita-15, Nishi-7, Sapporo 060-8638, Japan*
[4]*Robert Koch Institute, 13353 Berlin, Germany*
[5]*Institute for Zoo and Wildlife Research, 10252 Berlin, Germany*
[6]*Institute of Virology, Slovak Academy of Sciences, 84206 Bratislava, Slovakia*

Received March 22, 2004; Accepted July 14, 2004

Abstract. Seoul virus (SEOV) is a hantavirus causing a mild to moderate form of hemorrhagic fever with renal syndrome that is distributed mainly in Asia. The nucleocapsid (N) protein-encoding sequence of SEOV (strain 80-39) was RT-PCR-amplified and cloned into a yeast expression vector containing a galactose-inducible promoter. A survey of the pattern of synonymous codon preferences for a total of 22 N protein-encoding hantavirus genes including 13 of SEOV strains revealed that there is minor variation in codon usage by the same gene in different viral genomes. Introduction of the expression plasmid into yeast *Saccharomyces cerevisiae* resulted in the high-level expression of a hexahistidine-tagged N protein derivative. The nickel-chelation chromatography purified, yeast-expressed SEOV N protein reacted in the immunoblot with a SEOV-specific monoclonal antibody and certain HTNV- and PUUV-cross-reactive monoclonal antibodies. The immunization of a rabbit with the recombinant N protein resulted in the induction of a high-titered antibody response. In ELISA studies, the N protein was able to detect antibodies in sera of experimentally infected laboratory rats and in human anti-hantavirus-positive sera or serum pools of patients from different geographical origin. The yeast-expressed SEOV N protein represents a promising antigen for development of diagnostic tools in serology, sero prevalence studies and vaccine development.

Key words: codon usage, ELISA, hantavirus, monoclonal antibodies, nucleocapsid protein, Seoul virus, yeast expression

Introduction

Hantaviruses represent a separate genus *Hantavirus* in the family *Bunyaviridae*. They can cause two types of diseases in humans, "Hantavirus Cardiopulmonary Syndrome" (HCPS) in the Americas and "Hemorrhagic Fever with Renal Syndrome" (HFRS) mainly on the Eurasian continent [for reviews see [1,2]]. The prototype virus of the genus *Hantavirus*, the Hantaan virus (HTNV), carried by the striped field mouse (*Apodemus agrarius*), was identified as the causative agent of Korean Hemorrhagic Fever (KHF), a severe form

*Author for all correspondence:
E-mail: rainer.ulrich@wus.bfav.de
†Present address: Friedrich-Loeffler-Institut, Bundesforschungsinstitut für Tiergesundheit, Institut für Epidemiologie, D-16868 Wusterhausen, Germany

of HFRS, with a case fatality ratio of up to 10% due to severe bleeding, shock and renal failure [3,4]. Milder clinical courses of usually urban HFRS with a case fatality ratio of about 1% are caused by infections with the closely related Seoul virus (SEOV) carried by different species of the genus *Rattus*, i.e. *R. rattus*, *R. norvegicus* and *R. losea* [4–7].

In general, hantaviruses are transmitted from persistently infected rodent reservoir hosts to humans by inhalation of virus-contaminated aerosols originating from rodent excreta. In fact, data from experimental infection of urban rats (*R. norvegicus*) and investigations in an enzootic focus of SEOV-infected rats suggested the important role of virus-contaminated urine in the transmission of SEOV [8]. An additional transmission mode in male rats may be associated with aggression and wounding that is caused by increased testosterone levels [9].

SEOV infections have been reported from different Asian countries, i.e. Korea, China, Japan, (Far East) Russia, Indonesia and Cambodia [6,10–15]. However, SEOV is the only "cosmopolitan" hantavirus known so far and represents an example of global anthropogenic expansion of an infectious agent [16]. This is supported by the detection of human SEOV infections in other countries outside Asia, e.g. in the USA, Baltimore area [17] and Brazil [18], and circulation of SEOV in rat populations from Australia, USA, Germany, Northern Ireland, Indonesia and Greece [19–24]. Furthermore, infections by rat-borne hantaviruses have been reported in medical research institutions where laboratory rat colonies were handled [25]. In contrast, recent studies in Central Europe failed to detect human SEOV infections [26].

In general, diagnostics of human hantavirus infections is based on serological methods, i.e. immunofluorescence, ELISA and immunoblot tests. As an alternative to serological tests based on virus antigen or virus-infected cells, highly specific and sensitive tests were developed on the basis of heterologously expressed nucleocapsid (N) proteins. To prevent specificity problems associated with *E. coli*-expressed recombinant N (rN) protein [27], we have recently generated rN proteins of different hantaviruses, namely HTNV, different strains of Puumala virus (PUUV), Sin nombre virus (SNV), Andes virus (ANDV) and Dobrava virus strains associated to *Apodemus agrarius* (strain Slovakia; DOBV-Slk) and *A. flavicollis* (strain Slovenia; DOBV-Slo) in yeast *Saccharomyces cerevisiae* for use in diagnostic assays [28,29, J. Schmidt et al., submitted for publication].

The objective of the present study was the yeast expression and characterization of SEOV strain 80-39 rN protein for a potential use in diagnostic assays and vaccine applications. To prove if this rN protein can be taken in serological investigations as a representative of the SEOV species, the N protein-encoding sequence of Korean strain derivative 80-39-Berlin (80-39-B), cell culture-passaged in the biosafety level 3 laboratory in Berlin, was determined and its phylogenetic relationship to other SEOV strains was analyzed, most importantly to exclude a potential influence of nucleotide and resulting amino acid sequence alterations due to cell culture passaging. The purified SEOV rN protein was used to study its immuno-reactivity using monoclonal antibodies, sera of experimentally SEOV-infected rats, rabbits immunized with hantavirus rN proteins and human sera or serum pools from HFRS and HCPS patients.

Materials and Methods

Rat Sera und Tissue Samples

The generation of serial follow-up serum samples from four experimentally SEOV (strain SR-11)-infected Wistar rats has been described previously [30]. As negative control, sera from five wild-trapped rats from Japan, previously demonstrated to be non-infected [31], were used. In addition sera from 11 brown rats (*R. norvegicus*) trapped in Westphalia, Germany, were included in the study.

Total DNA from liver tissue samples of two wild-trapped brown rats from Germany was used for mitochondrial (mt) DNA characterization.

DNA Isolation, PCR Amplification and Determination of Rat mt DNA Sequences

Total rat DNA was isolated using the QIAamp DNA Mini Kit according to the protocol of the manufacturer (QIAGEN, Hilden, Germany). The 12S rDNA sequence was PCR-amplified using the

primers L1091 (5′-GGGATTAGATACCCCAC-TAT-3′) and H1478 (5′-TGACTGCAGAGGGT-GACGGGCGGTGTGT-3′) from the isolated rat DNA and sequenced using the ABI Prism Big Dye terminator cycle sequencing kit (Applied Biosystems, Foster City, CA) according to the manufacturer's protocol on ABI 377 DNA sequencers.

RNA Isolation, RT-PCR, Cloning and Sequencing of the SEOV N Protein-encoding Sequence

Vero E6 cells were infected with SEOV (strain 80-39) [5]. Infected cells as well as cell culture supernatant were treated with Trizol reagent (Gibco BRL, Eggenstein, Germany). The suspensions were used to isolate viral RNA with the RNeasy Kit (QIAGEN), according to the recommendations of the manufacturer. After reverse transcription of the RNA by RevertAid H Minus M-MuLV Reverse Transcriptase (MBI Fermentas, St. Leon-Rot, Germany) with the Seoul-S-RT Primer 5′-TAGTAGTAGACTCCCT AAA-GAGCTA-3′, the N protein-encoding sequence (aa 2-429) of the cDNA copy was PCR-amplified using Pfu DNA Polymerase (Stratagene, Amsterdam, The Netherlands) with the SEOV-N Forward Primer 5′-AAGCTAGCGCAACTATG GAAGAAATCCAGAGAG-3′ and the SEOV-N Reverse Primer 5′-AAGCTAGCTTATAATTTC ATAGGTTCCTGGTTTGA-3′, containing unique sites for *Nhe*I. The PCR amplification products were purified and subsequently inserted into the plasmid pSTBLUE-1 with the Perfectly Blunt Cloning Kit (Novagen, Schwalbach, Germany), according to the recommendations of the manufacturer. Plasmids were purified using the Spin Mini Kit (QIAGEN). DNA sequencing of three plasmids was performed using an ABI Prism Big Dye terminator cycle sequencing kit (Applied Biosystems). The N protein-encoding sequences obtained for three pSTBLUE-1/SEOV-N plasmids were identical.

Codon Use Analyses

The DnaSP 4.0 program [32] was used to calculate codon usage tables as well as the G + C content at the second (G + C2), third (G + C3), and all coding positions (G + Cc) for each N protein-encoding sequence analysed. The same program was also used to calculate different codon bias measures: the Relative Synonymous Codon Usage (RSCU; [33]) values, the Effective Number of Codons (ENC; [34]), the Codon Bias Index (CBI; [35], and the Scaled Chi square (SChi2; [36]) values. To examine the similarities of a set of genes in terms of their similarity of codon usage, we followed McInerney's approach implemented in the GCUA program [37]. A distance matrix was produced from all the N protein-encoding sequences based on the average differences in their RSCU values. The analysis was continued with a tree-like representation of this RSCU distance matrix produced using PAUP* and comparing that to the ML phylogeny of the sequences based on a substitution model.

Phylogenetic Analysis of Nucleotide and Amino acid Sequences

For phylogenetic analysis, the sequences were aligned on amino acid level and then reverse-translated to nucleotide sequences using DAMBE software [38]. DotPlot analysis implemented in BioEdit software package [39] was used to check the reliability of the alignment. We carried out two types of phylogenetic analysis to investigate evolutionary relationships using PAUP* 4.0b10 [40]: (i) neighbour-joining (NJ) based on LogDet/paralinear distances which were designed to deal with unequal base frequencies in each pairwise sequence comparison – thus it allows base compositions to vary over the tree [41] and (ii) maximum-likelihood (ML) analysis. Before the ML analyses, we used likelihood ratio tests and the computer application MrModeltest v1.0b. [42] to determine the best-suited model of sequence evolution. The best-fit model selected by MrModeltest v1.0b. for the N protein-encoding sequence data set and then used to reconstruct phylogenetic trees was the general time-reversible model [43] with an allowance for invariant sites and a gamma shape for among-site rate variation under the hierarchical likelihood ratio test method. Heuristic ML searches were performed with 10 replicates of random sequence addition and TBR branch swapping. Non-parametric bootstrap analyses with 100 pseudo-replicates were performed to obtain estimates of support for each node of the ML tree; NJ bootstraps employed 1000 iterations.

Generation of the Yeast Expression Plasmid

The SEOV-N-encoding sequence was isolated from pSTBLUE-1/SEOV-N as an *Nhe*I fragment and inserted into *Xba*I-linearized, CIP-dephosphorylated plasmid pFX7-His. This plasmid represents a derivative of pFX7 that contains a Gal/Pyk hybrid promoter, a formaldehyde resistance gene and in front of the unique *Xba*I insertion site an MHHHHHH-coding sequence [28,29]. The DNA sequence in the joining region of pFX7-His plasmid and the SEOV N-encoding insert in the expression plasmid pFX7-His-SEOV-N was confirmed by DNA sequencing using primer pyk5 (5′-TTCTTTTTCATCCTTTGG-3′).

Expression and Purification of SEOV rN protein

The recombinant plasmid pFX7-His-SEOV-N was introduced into competent yeast *S. cerevisiae* cells of the haploid strain AH22 derivate 214 (*ura3 leu2 his4*). Expression and purification of the His-tagged rN protein was performed according to a protocol described recently for rN proteins of other hantaviruses [28,29]. Briefly, yeast cells were grown in formaldehyde-containing YEPD medium. Synthesis of the SEOV rN protein was induced by adding galactose. Yeast cells were pelleted by centrifugation and disrupted using glass beads. The His-tagged SEOV rN protein, enriched by centrifugation steps, was finally purified using nickel-chelate resin according to the protocol of the manufacturer (QIAGEN). The rN proteins of PUUV strains Vranica/Hällnäs (PUUV-Vra), Kazan (PUUV-Kaz) and Sotkamo (PUUV-Sot), HTNV (strain Fojnica), SNV and ANDV were purified according to the same protocol.

Human Sera and Serum pools

An anti-SEOV human serum and two anti-HTNV human sera originated from the Republic of Korea. The anti-DOBV and anti-PUUV serum pools were each generated from four routine diagnostic serum samples of German HFRS patients regarded as positive for anti-DOBV-IgG and anti-PUUV-IgG, respectively, by in-house mAb-capture ELISA and Western blot tests based on yeast-expressed DOBV and PUUV rN proteins [Meisel et al., unpublished data] and chemiluminescence focus reduction neutralization assays [44]. The anti-SNV pool contained 15 routine diagnostic serum samples of HCPS patients from the US found to be anti-SNV-IgG positive by SNV strip blot assay [45] and our in-house SNV-IgG ELISA and Western blot tests using yeast-expressed SNV rN protein (J. Schmidt et al., submitted for publication]. For preparation of an anti-ANDV pool 56 anti-ANDV-IgG-positive serum samples derived from Argentinean and Chilean HCPS patients were used which were confirmed to be reactive by in-house SNV- or ANDV-IgG ELISA and Western blot tests [46,47, J. Schmidt et al., submitted for publication]. As a control a negative serum pool was generated from German serum samples of our routine diagnostics found to be negative for anti-HTNV-, anti-DOBV-, anti-PUUV-, anti-SNV- and anti-ANDV-IgG by our in-house ELISA tests based on the corresponding yeast-expressed rN proteins (29, Schmidt et al., submitted for publication].

Immunization of Rabbits with Yeast-expressed Hantavirus N Proteins

Three rabbits were immunized subcutaneously three times with an interval of 2–4 weeks with 100 µg of one of the purified His-tagged, yeast-expressed rN proteins of SEOV, SNV or ANDV dissolved in PBS. Blood samples were taken 1 week after booster immunization and up to 3 weeks later. After clotting of the blood and centrifugation the sera were stored at −20°C until use. The generation of HTNV- and PUUV-Sot-rN protein-specific rabbit sera followed the same protocol as has been described recently [29].

SDS-Polyacrylamide Gel Electrophoresis (SDS–PAGE) and Western Blot

SDS–PAGE and Western blot analysis were performed as described recently [29]. Aliquots of 2 µg of each purified rN protein of SEOV, ANDV, SNV, PUUV-Vra, PUUV-Sot, PUUV-Kaz and HTNV were run on a 12.5% SDS polyacrylamide gel and electro-blotted to nitrocellulose membrane. After blocking, the membranes were incubated overnight at room temperature (RT) with a panel of N-specific monoclonal antibodies (mAbs)